



Scholars Research Library

Archives of Applied Science Research, 2010, 2 (5):298-310

(<http://scholarsresearchlibrary.com/archive.html>)



ISSN 0975-508X

CODEN (USA) AASRC9

## Mechanical and thermal studies of pure and KOH doped glycine phosphite single crystals: Sankaranarayanan–Ramasamy (SR) method

S. Supriya and S. Kalainathan\*

School of Advanced Sciences, VIT University, Vellore, India

### ABSTRACT

The single crystals of pure glycine phosphite (pure-GPI) and potassium hydroxide doped glycine phosphite (KOH-GPI) were grown by slow evaporation and Sankaranarayanan and Ramasamy (SR) method. Colourless crystal with cylindrical shape about maximum diameter of 18 mm and 28 mm length was obtained within a month. The morphologies were analyzed for the pure and KOH-GPI crystals which are grown by slow evaporation method. For both the crystals the crystal system was found to be monoclinic based on the single crystal X-ray diffraction analysis. The crystalline quality has been analyzed for both the compounds by the powder X-ray diffraction studies. From differential thermal analysis data of both the compounds were compared. From Vickers indentation method, Meyer's index number ( $n$ ) and hardness value of the crystal was calculated. Young's modulus, anisotropy nature of the crystal and Brittleness property were analyzed for both the samples.

**Keywords:** Growth from solution; X-Ray diffraction; microhardness.

PACS:- 81.10.Dn; 61.05.cp; 62.20.Qp

### INTRODUCTION

The  $\alpha$ -amino acid glycine gives number of inorganic materials which are having good dielectric and elastic properties. The second hydrogen bonded ferroelectric crystal of phosphorous acid with an amino acid is known as glycine phosphite ( $\text{NH}_2\text{CH}_2\text{COOH}_3\text{PO}_3$ ), abbreviated as GPI, and betanine phosphite crystals [ $(\text{CH}_3)_3\text{NCH}_2\text{COOH}_3\text{PO}_3$ ], abbreviated as BPI are related to the ordering of protons in their structure. The GPI crystal belongs to monoclinic system with space group P21/a and cell parameters of  $a = 9.792 \text{ \AA}$ ,  $b = 8.487 \text{ \AA}$  and  $c = 7.411 \text{ \AA}$  and  $\beta = 100.43^\circ$  [1,2]. In low temperature phase GPI shows spontaneous polarization along the b-axis, and proton ordering is expected along c-axis. At 224 K it shows ferroelectric to para-electric phase

transition [3-5]. To understand the mechanism of ferroelectric to para-electric phase transition many researchers have grown these GPI crystals [6-8].

In this work we adopted the novel technique known as Sankaranarayanan and Ramasamy method (SR method) to grow the new crystal named potassium hydroxide doped glycine phosphite (KOH-GPI). This solution growth method is the best one than the other methods. It is having advantage of less sophisticated instrumentation and easy handling [9-11]. Crystals of different morphology and different orientations are grown by conventional solution growth techniques but for good applications the crystal with specific orientation and good quality is needed for us. By this SR method the crystal can be grown with specific orientation. Also this method is having major advantage that the entire solution can be converted into crystal that 100% solute-crystal efficiency can be achieved [12,13].

In this work we have grown 5 mole % of KOH doped glycine phosphite single crystal by SR method, which is not reported in literature so far.

## MATERIALS AND METHODS

### 2.1 Material synthesis and growth of KOH doped GPI by Slow evaporation method

The chemicals of glycine [NH<sub>2</sub>CH<sub>2</sub>COOH] (AR grade) and orthophosphorous acid [H<sub>3</sub>PO<sub>3</sub>] (Sigma Aldrich) were taken in 1:1 ratio to obtain pure glycine phosphite (GPI) compound. These chemicals were weighed and mixed in millipore water solvent. The following reaction is expected to take place for the formation of glycine phosphite.



In the millipore water solvent the glycine and orthophosphorous acid were completely dissolved. After this complete dissolution the 5 mole % of potassium hydroxide (KOH) was added as a dopant material in this solution. This solution was heated slowly upto 80°C so that all the chemicals were dissolved completely. The transparent solution was obtained and the temperature of the solution was decreased gradually to the room temperature. Afterwards this solution was kept in refrigerator and it was cooled to 0°C. After complete precipitation and by doing proper filtering, the dried KOH-GPI chemical powder was obtained. The KOH doped GPI synthesized salt was recrystallized several times to get purified material and good quality crystals. By employing the slow evaporation technique, the fine crystals of KOH-GPI were obtained from saturated solution.

Pure GPI crystals were also grown similarly by slow evaporation and SR methods (the following method) without adding potassium hydroxide.



## 2.2 Growth of KOH doped GPI single crystal by SR method

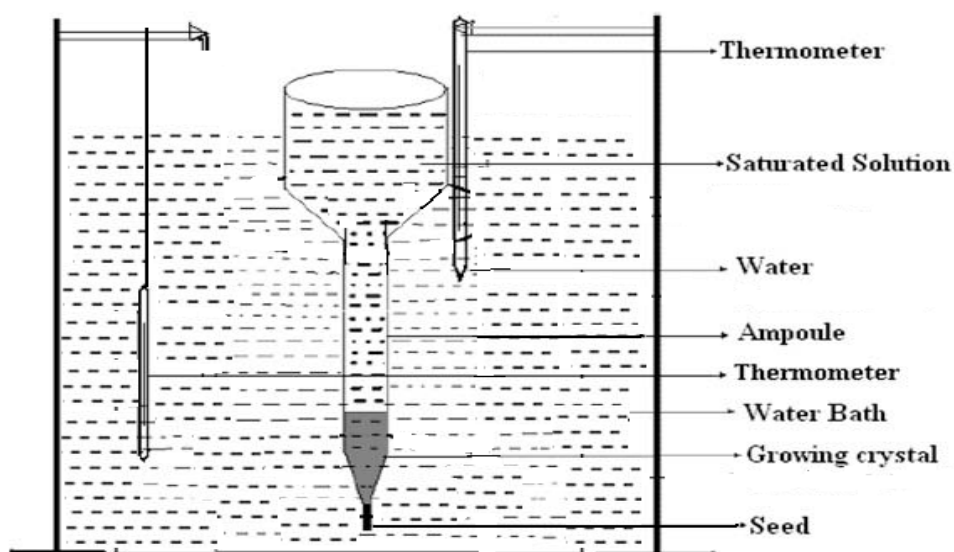


**Figure. 3 Schematic diagram of SR set up**

The crystal which is obtained from slow evaporation technique is inserted to the growth ampoule which contains saturated solution of KOH-GPI. The growth ampoule is made out of glass and consisting seed mounting pad at the bottom. A ring heater is placed on the top of growth ampoule and it is connected with temperature controller so that it provides necessary temperature for the solvent evaporation. The whole experimental setup was placed in dust free hood. The schematic diagram of the experimental setup is shown in Fig. 3. The crystal which is obtained by slow evaporation method was allowed to grow for required length under proper temperature controlled condition. The growth of crystal was directly observed because of its transparent nature of solution and the growth ampoule. Under controlled temperature condition the potassium hydroxide doped glycine phosphite single crystal with size of 18 mm diameter and 28 mm length was obtained with in a month which is shown in Fig. 4.



**Figure. 4 KOH-GPI crystal by SR method**

### 3. Characterization studies

The lattice parameter and crystal system of the pure and KOH doped GPI crystal was confirmed by single crystal X-ray diffraction analysis using ENRAF NONIUS CAD4 diffractometer. The powder samples of the both the crystals have been analyzed by using Rich seifort (model 2002) X-ray diffractometer. The differential thermal analysis (DTA) were carried out by using SHIMADZU DT-40 simultaneous DT analyzer with a heating rate of 10° C/min. The Vicker's and Knoop microhardness measurement of the crystal was observed using Mitutoyo MH 120 microhardness tester.

## RESULTS AND DISCUSSION

### 4.1 Single crystal X-ray diffraction analysis

**Table. 1 Cell parameter details from single crystal X-ray diffraction**

	a (Å)	b (Å)	c (Å)	β(°)
<b>Pure GPI</b>	9.782	8.482	7.402	100.33
<b>KOH-GPI</b>	9.911	8.891	7.812	100.74

$\alpha = \gamma = 90^\circ$   
 Volume = 606.08 Å<sup>3</sup>  
 System = monoclinic

The lattice parameter and crystal system of KOH-GPI crystal was calculated by single crystal X-ray diffraction analysis and compared with pure GPI. These values which we obtained for pure GPI is almost similar with reported values of GPI [15]. The table 1 shows the lattice parameters values of pure GPI and KOH-GPI. The results reveal that KOH-GPI also belongs to monoclinic system with the space group P21/a.

### 4.2 Powder X-ray diffraction analysis

To confirm the quality of crystal and crystalline structure the powder samples have been analyzed by powder X-ray diffraction. The powder samples pure and KOH doped GPI were subjected to intense X-rays of 1.5418 Å (CuKα) at a scan speed of 2° per minute. Fig. 5 shows the powder X-ray diffraction pattern of pure and KOH doped GPI crystal. Comparing with pure GPI there is missing of some peaks and also change in intensity of peaks is clearly visible due to addition of KOH with GPI. The observed results are in good agreement with the reported results of pure GPI [15].

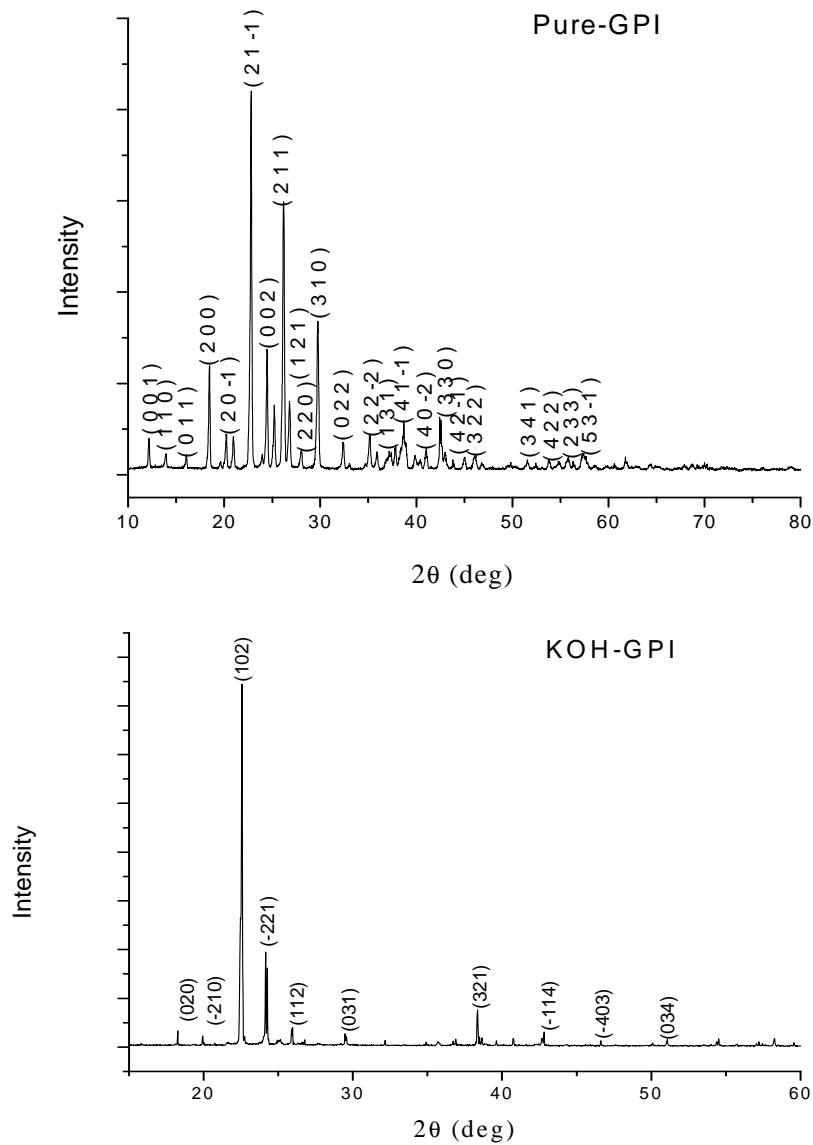


**Figure. 5 Powder X-ray diffraction pattern of pure and KOH doped GPI**

#### 4.3 Thermal analysis

The thermal stability of pure and KOH doped GPI was analyzed by using differential thermal analyzer (DTA). From Fig. 6 the DTA curve shows the endothermic peak corresponding to melting point of pure and KOH doped GPI and followed by

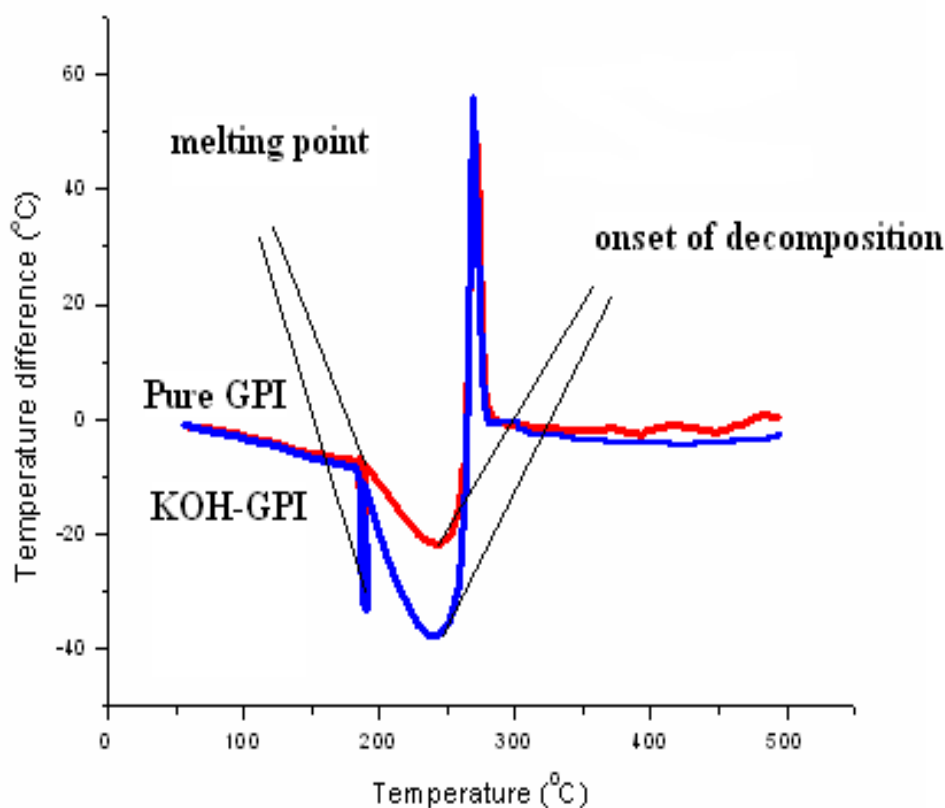


**Figure. 6 DTA curve**

stepwise decomposition of both the materials. The thermal data of KOH-GPI was compared with pure GPI. Both the samples show the sharp endothermic DTA peak at 180° C corresponds to the melting point of the sample and the exothermic DTA peak immediately following the melting point can be due to stepwise decomposition of the materials [16].

#### **4.4 Microhardness studies**

The crack free crystal having approximate dimensions of 4 mm x 3 mm x 2 mm (pure GPI) and 4 mm x 2 mm x 1 mm (KOH-GPI), with flat and smooth faces, were chosen for the indentation test. The polished surface of the crystals were indented gently by the loads varying from 10 to 50 g for a dwell period of 10 s by using Vicker's and Knoop indenter which are attached to an incident ray research microscope.

#### 4.4.1 Vicker's microhardness

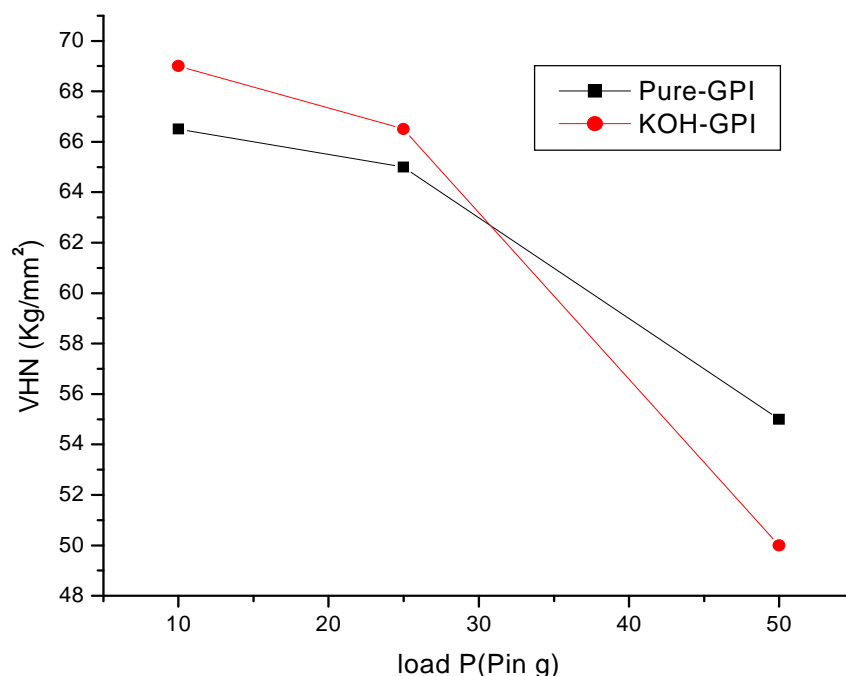


**Figure. 7** Plot of Vickers hardness number ( $H_v$ ) Vs load ( $P$ ).

The Vicker's microhardness measurements were done for different forces. The micro hardness was evaluated by applying indentation in the surface of pure and KOH doped GPI crystal. The hardness was calculated using for the applied loads of 10, 25 and 50g using the relation

$$H_v = 1.8544 P/d^2 \text{ kg/mm}^2$$

Where,  $H_v$  is the Vicker's microhardness,  $P$  is the applied load,  $d$  is the diagonal length of the indentation. For a load of the 100 g, the cracks started developing around the indentation mark. The graph was plotted between Vicker's hardness number ( $H_v$ ) Vs applied load ( $P$ ) which is shown in the Fig. 7.

Fig. 8 explains the relation between  $\log P$  Vs  $\log d$  fitting data before cracking after least square fitting gives the straight line graph for both the samples. The Vicker's hardness value of pure GPI is compared with hardness value of KOH-GPI. The KOH-GPI Vicker's hardness value is increased comparing with pure GPI which is shown in the table 2.

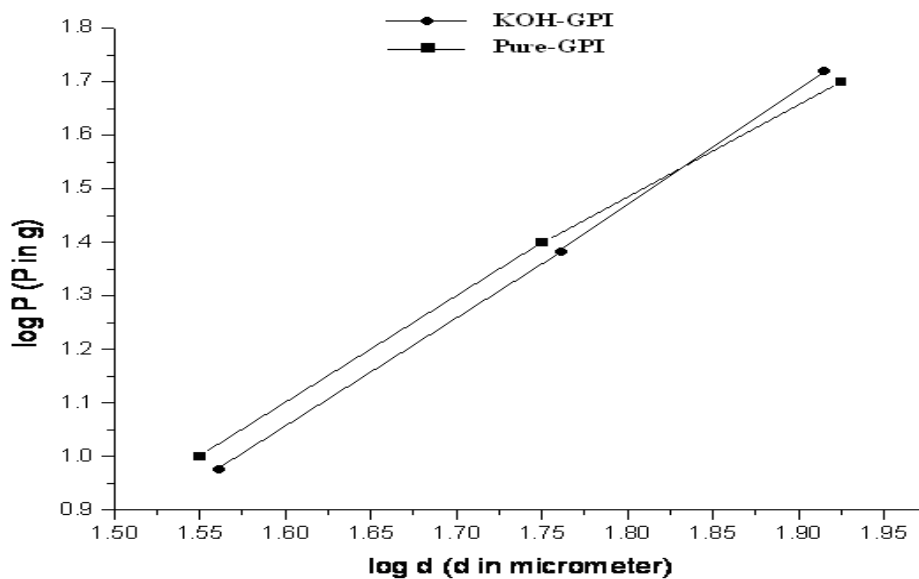


**Figure. 8 Plot of log P Vs log d**

**Table. 2 Hardness value of pure and KOH doped GPI crystals**

S. No.	Crystal Name	H <sub>v</sub> for the load 10g
1.	Pure GPI	66.5
2.	KOH-GPI	69

Straight line graph shows good agreement with Meyer's law. The value of  $n$  is found from the slope of the graph and it was found to be 1.625 for KOH-GPI which shows harder than pure GPI. According to Onitsch and Hanneman the 'n' should lie between 1 and 1.6 for the hard materials and above 1.6 for softer ones [16]. The value of KOH-GPI also shows that it belongs to soft material category.

#### 4.4.2 Knoop microhardness

The initiation of crack and materials chipping become significant beyond 50 g of the applied load. So beyond this load the hardness measurement could not be carried out. From this measurement it was observed that the load increased upto 50 g, the knoop microhardness number decreases with load.



**Figure. 9** Indentation mark of knoop’s microhardness

Fig. 9 shows the photograph of the indentation mark of knoop microhardness which was performed in the surface of the KOH-GPI crystal.

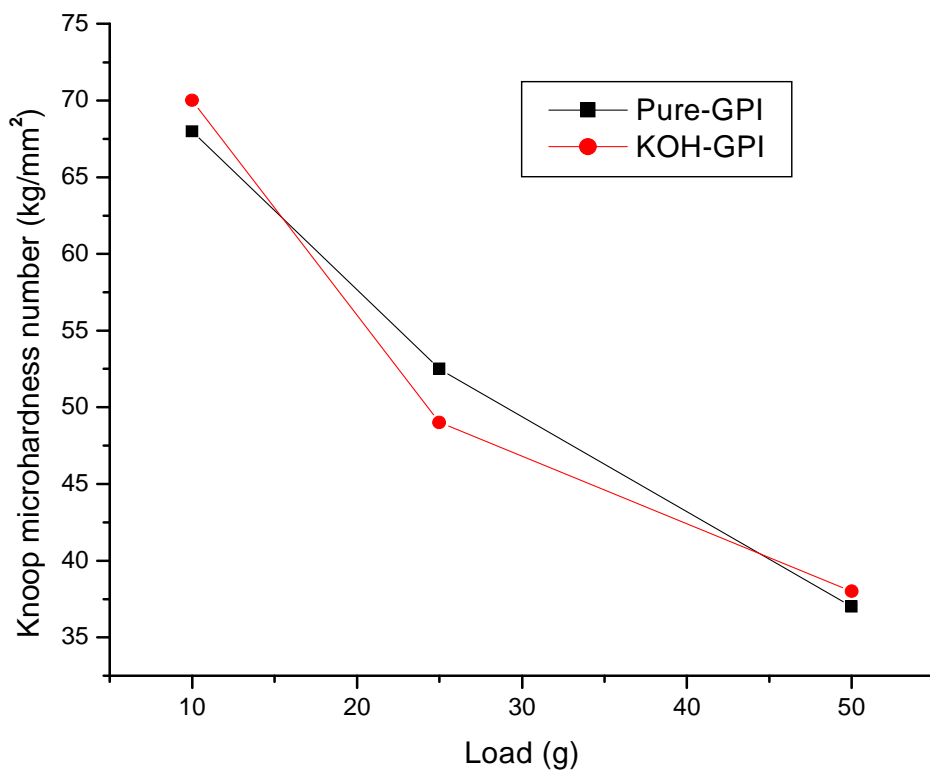


**Figure. 10** Variation of Knoop microhardeness with load

The graph was plotted against knoop hardness ( $H_k$ ) Vs load (P) for pure and KOH doped GPI. The plot is shown in Fig. 10. From the knoop microhardness measurements the Young's modulus (E) of the crystals were calculated using the relation [17].

$$E = 0.045H_k / (0.1406-b/a)$$

Where  $H_k$  is the knoop microhardness value at a particular load, b and a are the shorter knoop indentation diagonal and the longer indentation diagonal respectively.

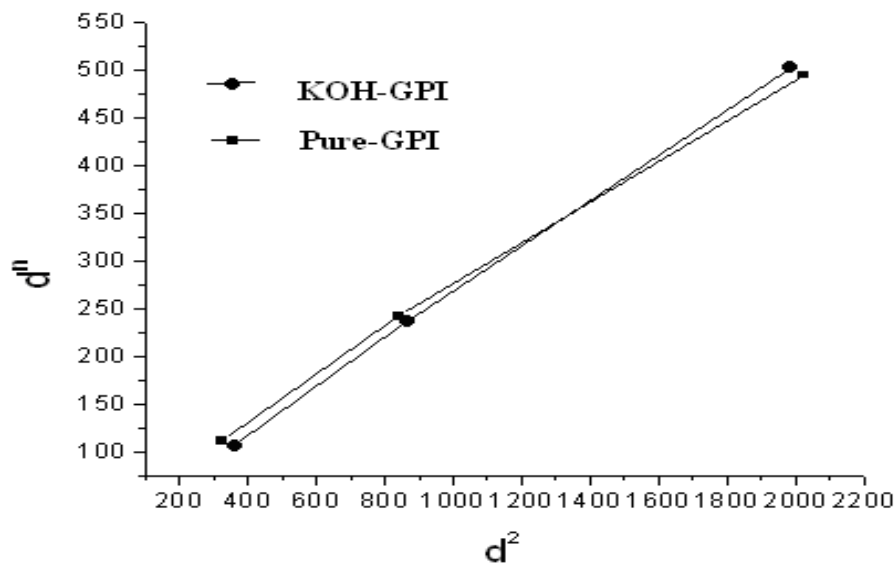


**Figure. 11 Plot of  $d^2$  Vs  $d^n$**

According to Heys and Kendall' formula the value of  $d^n$  was calculated (for both the samples) and the graph was plotted against  $d^2$  and  $d^n$  which gives a straight line as shown in the Fig. 11 [18]. For pure and KOH doped GPI the Young's modulus was calculated as  $1.35 \times 10^{10} \text{N/m}^2$  and  $1.312 \times 10^{10} \text{N/m}^2$  respectively.

#### 4.4.3 Anisotropy nature

To study anisotropic nature of both the crystals, the microhardness was measured by varying the crystal orientation over the range of  $0^\circ$ –  $360^\circ$  in steps of  $30^\circ$ . No distortion in the shape of the indentation was observed with the crystal orientation. From

Fig. 12, the maximum hardness number ( $H_k \text{ max}$ ) was observed at equal intervals ( $0^\circ$  to  $360^\circ$ ). The variation in hardness number indicates the anisotropic nature of both the crystals. The crystal structure and the slip system play an important role in the observed variation of hardness with crystal orientation. The directional variation in hardness might be due to the change in orientation of the slip system of the crystal with respect to the indenter.

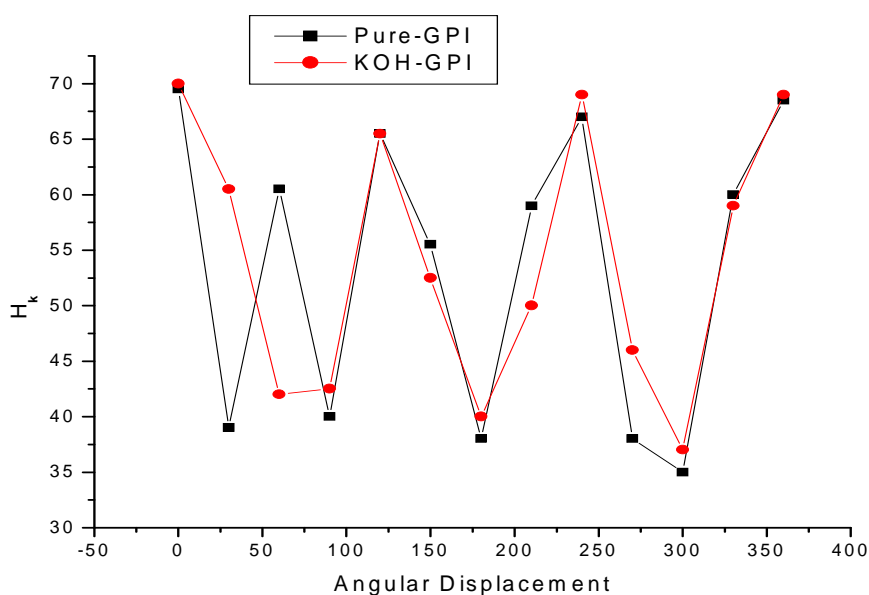


**Figure. 12 Anisotropy nature**

#### 4.4.4 Brittleness index

The value of brittleness index  $B_i$  is calculated using the following relation

$$B_i = H_v / K_c$$

Brittleness is an important property that affects the mechanical behavior of a material and fracture induced in a material without deformation. The value of  $K_c$  [18] was calculated as 0.1279 and 0.1281  $\text{MNm}^{-3/2}$  for pure and KOH doped GPI respectively. For pure GPI the  $B_i$  was found to be 4860.05  $\text{m}^{-1/2}$  and for KOH doped GPI it was calculated as 4839.99  $\text{m}^{-1/2}$ . According to the published scale for estimating the brittleness number of crystals, the cracks obtained around any single indentation impression gives one of the five standards of brittleness as reported in the literature. This indentation impression leads to the conclusion that the GPI crystal shows a brittleness of 1–4 standards. Brittleness number of the order of 5 should not be used for determining microhardness values [18,19].

## CONCLUSION

The pure and 5 mole % KOH doped glycine phosphite single crystal was grown by slow evaporation and SR method and its morphology has been analyzed. From thermal data the melting point and decomposition of the both the samples were analyzed. The Vickers and Knoop microhardness number ( $H_v$  and  $H_k$ ) was calculated for pure and KOH doped GPI. The Young's modulus was calculated from the diagonal lengths of Knoop's indentation. The variation in hardness for the both the crystals exhibits anisotropic property. Brittleness index number of the both the crystals has been calculated.

**Acknowledgements**

Authors are thankful to management of VIT University, Vellore for their constant financial assistance and encouragement.

**REFERENCES**

- [1] T. Ishibashi, M. Machida, *J. of the Phy. Soc. of Jap.*, **2003**, 72, 1554.
- [2] S. Kalainathan, M. Beatrice Margaret, *Mat. Sci. and Engg B.*, **2005**, 120,190.
- [3] M. Sledź, J. Baran, *J. Mol. Structure.*, **2004**, 706, 15.
- [4] J. Baran, K. Lukaszewicz, A. Pietraszko, M. Sledz, *J. Mol. Struc.*, **2002**, 611,155.
- [5] J.Tritt-Goc, N. Pislewski, L. Szczepanska, R. Goc, *Solid State Commun.*, **1998**,108,189.
- [6] C. Preethy Menon, J. Philip, A. Deepthy, H. L. Bhat, *Mat. Res. Bulle.*, **2001**,36, 2407.
- [7] S. Dacko, Z. Czaplá, J. Baran, M. Drozd, *Phys. Lett. A.*, **1996**, 223, 217.
- [8] J. Goslar, S.K. Hoffmann, W. Hilczer, *Solid state commun.*, **2002**, 121, 423.
- [9] P. Ramasamy, *J. of Cry. Grow.*, **2008**, 31,1501.
- [10] K. Sankaranarayanan, P. Ramasamy, *J. of Cry. Grow.*, **2006**, 292, 445.
- [11] S. Balamurugan, P. Ramasamy, Y. Inkong, P. Manyum, *Mat. Chem. and Phy.*, **2009**,113, 622.
- [12] K. Sethuraman, R. Ramesh Babu, R. Gopalakrishnan, P. Ramasamy, *J. of Cry.Grow.*, **2006**, 294, 349.
- [13] M. Senthil Pandian, N. Balamurugan, V. Ganesh, P.V. Raja Shekar, K. Kishan Rao, P. Ramasamy, *Mat. Lett.*, **2008**, 62, 3830.
- [14] J. Nayeem, T. Kikuta, T.Yamazaki, N. Nakatani, *Jpn. J. of App. Phy.*, **2000**, 39, 6612.
- [15] S. Kalainathan, R. Ezhil Vizhi, M. Beatrice Margret, *Ferroelec.*, **2006**, 332, 21.
- [16] A. Deepthy, H.L. Bhat, *J. of Cry. Grow.*, **2001**, 226, 287.
- [17] T. Pal, T. Kar, *Mat. Lett.*, **2005**, 59,1400.
- [18] K. Nihara, R. Morena, D.P.H. Hasselman, *J. Mater. Sci. Lett.*, **1982**,1,13.
- [19] N.A. Goryunova, A.S. Borshchevskii, D.N. Tretiakov, *Hardness Semiconductor and Semimetals*, New York, Academic Press, **1968**, 3, 25.